Persistent homology derived radiomic feature predicts survival in non-small cell lung cancer patients treated with SBRT

Eashwar Somasundaram[1,*], Raoul R. Wadhwa[2], Adam Litzler[3], Rowan Barker-Clarke[4], Peng Qi[5], Gregory Videtic[5], Kevin Stephans[5], Nathan A. Pennell[6,10], Daniel Raymond[7], Kailin Yang[5], Michael W. Kattan[8,10], and Jacob G. Scott[4,5,9,10 +]

[1]Case Western Reserve University School of Medicine, Cleveland, OH 44195, USA
[2]Cleveland Clinic Lerner College of Medicine, Case Western Reserve University, Cleveland, OH 44195, USA
[3]University of Colorado Boulder, Department of Applied Mathematics, Boulder, CO 80309, USA
[4]Lerner Research Institute, Department of Translational Hematology and Oncology Research, Cleveland Clinic, Cleveland, OH 44195, USA
[5]Taussig Cancer Institute, Department of Radiation Oncology, Cleveland Clinic, Cleveland, OH 44195, USA
[6]Taussig Cancer Institute, Department of Hematology Oncology, Cleveland Clinic, Cleveland, OH 44195, USA
[7]Heart and Vascular Institute, Department of Thoracic and Cardiovascular Surgery, Cleveland Clinic, Cleveland, OH 44195, USA
[8]Lerner Research Institute, Department of Quantitative Health Sciences, Cleveland Clinic, Cleveland, OH 44195, USA
[9]Case Western Reserve University School of Medicine, Department of Systems Biology and Bioinformatics, Cleveland, OH 44195, USA
[10]Case Comprehensive Cancer Center, Cleveland, OH 44195, USA
[*]Email: evs27@case.edu
[+]Correspondence: scottJ10@ccf.org; 9500 Euclid Ave Desk NE-6, Cleveland, OH 44195, United States.

ABSTRACT

Introduction: Predicting survival in NSCLC is a goal of clinicians in guiding therapy, trialists in risk stratifying patients, and patients for prognosis counseling. Traditional risk calculators for survival use clinical and histopathologic data to predict survival. We propose incorporating the PHOM (persistent homology) score, the radiomic quantification of solid tumor topology, to predict overall survival.

Methods: Patients diagnosed with stage I or II NSCLC and status post definitive SBRT treatment were selected ($n = 554$). The PHOM score was calculated on each patient's pre-treatment CT scan. PHOM score, age, sex, stage, KPS, CCI, and post-SBRT chemotherapy were predictors in the generated Cox proportional hazards models for overall and cancer-specific survival. Patients were split into high and low PHOM score groups by median value and compared using KM curves for overall survival and cumulative incidence curves for cause specific death. Optimized tertile PHOM risk groups were calculated and similarly compared for overall survival and cause-specific death. Internal validation was conducted with bootstrap resampling and calibration curves were checked. Finally, a nomogram to predict overall survival was generated and is publicly available at https://eashwarsoma.shinyapps.io/LungCancerTDATest/.

Results: PHOM score was a significant predictor for overall survival (HR: 1.17, 95% CI: $1.07-1.28$) and was the only significant predictor for cancer-specific survival (1.31, 95% CI: $1.11-1.56$) in the multivariable Cox model. The median survival for the high PHOM group was 29.18 months (95% CI: $23.62-34.27$), which was significantly worse compared to the low PHOM group (45.41 months, 95% CI: $40.08-51.78$, $p < 0.001$). The high PHOM group had a significantly greater chance of cancer-specific death at post treatment month 65 (0.244, 95%CI: $0.192-0.296$) compared to the low PHOM group (0.171, 95% CI: $0.123-0.218$, $p = 0.029$). Nomograms for 1, 2, 5, and 8-year overall survival were successfully calibrated using the Cox model.

Conclusions: The PHOM score is associated with cancer-specific survival and predictive of overall survival. Our developed nomogram can be used to inform clinical prognosis and assist in making post-SBRT treatment considerations.

Conflicts of Interest
The authors have no conflicts of interest to disclose, financial or otherwise, in relation this article.

Funding
JGS was supported by NIH grant R37 CA244613 and American Cancer Society. ES and RRW were supported by the Case Comprehensive Cancer Center Summer Training Grant for medical students. KY was supported by the Computational Genomic Epidemiology of Cancer (CoGEC) Program at Case Comprehensive Cancer Center (T32CA094186), Young Investigator Award from ASCO Conquer Cancer Foundation, and RSNA Research Resident Grant.

Keywords: non-small cell lung cancer, predictive model, radiomics, persistent homology, nomogram

1 Introduction

Approximately 230,000 cases of lung cancer are diagnosed and 135,000 patients die from lung cancer each year in the US[1]. Proportionally, 85% of all lung cancer cases are non-small cell lung cancer (NSCLC)[2]. Primary therapy has traditionally been surgical resection; however, stereotactic body radiation therapy (SBRT) is now an option for patients with inoperable tumors[3]. For all cancers, clinical prognostication is essential for therapy selection. This is especially important in lung cancer, for which 5-year survival is highly variable in NSCLC ranging from nearly 70% for patients with stage I disease down to 10% for patients with metastatic disease[4].

Risk calculators are clinical decision support tools that quantify clinical prognosis. They typically use patient-specific histopathologic and clinical covariates to predict outcomes. Risk calculators incorporating molecular and clinical information have been developed for lung cancer[5]. Although clinical data is easy to obtain and incorporate in such risk models, collecting detailed molecular information often poses a challenge outside of tertiary medical centers. Imaging data is far more readily accessible. Radiomics - the science of extracting and analyzing features from imaging data - has been increasingly used to predict clinical outcomes in cancer[6]. While radiomics already offers a wide toolset for image analysis, we propose a valuable extension with persistent homology.

Persistent homology quantifies the global topology, or overall shape, of big data[7]. Analogously in the histologic context, oncology already features qualitative shape analysis through Gleason scoring to grade prostate cancer severity based on gland shape[8]. These high-level approaches provide the clear benefit of discriminating signal from noise. We believe that malignant and benign tissue exhibit distinct topology on clinical imaging. Widely used heuristics in clinical medicine support this intuition. For instance, malignant tumors are typically diffusely spread, heterogeneous in composition, and may possess necrotic cavities. On the other hand, benign tumors are usually well-circumscribed and more likely to be homogeneous in appearance[9]. Persistent homology formalizes and quantifies these observations to permit their use in predictive models. Of note, persistent homology has already been introduced to radiomics in the study of glioblastoma and liver cancer[10,11].

Even within lung cancer, persistent homology has shown promise in predictive modeling via a metric named the PHOM score, which quantifies the texture of a solid tumor based on CT imaging data[12]. In our previous study, we demonstrated that the PHOM score is associated with overall survival. We hypothesize that the PHOM score can predict survival associated with NSCLC treated with SBRT. Here, we validate and extend the PHOM score using a large prospectively collected, IRB approved dataset from our institution including 554 patients treated with SBRT for primary lung cancers from 2008-2019. We combine our PHOM score with clinical covariates to develop prognostic nomograms that predict duration of overall survival post-diagnosis. Our validated PHOM score has the potential to stratify patients into risk categories, which can be useful for both future clinical trial stratification and treatment selection.

2 Materials and Methods

We developed a data pipeline that calculated the PHOM score of computed tomography (CT) tumor scans, generated regression models, and internally validated these models to predict survival. Methodology to generate a PHOM score using tumor CT scans is described in our previous work[12]. Only patients with early stage (I or II) biopsy proven primary non small cell lung cancer with no prior treatment history were eligible for this study. We utilized a prospectively collected dataset of CT scans for patients receiving SBRT entailing 803 patient scans with corresponding clinical data. After excluding 249 patients with metastatic disease, nodal disease, additional primary tumors, and patients who received pretreatment, 554 patients met inclusion criteria (**Figure 1A**) All patients received SBRT therapy as their primary treatment for local control.

Each patient's primary lung tumor had been segmented by a radiation oncologist. For each lung tumor CT scan, we used the segmentation coordinates to crop the tumor CT scan to only include tumor tissue. A PHOM score was calculated from this data object (**Figure 1B**). As previously described, this metric reflects the number of disconnected foci of pixels with similar gray scale values in the segmented tumor object[12].

We demonstrate PHOM's potential clinical utility through a Cox Proportional Hazards model and nomogram (**Figure 1C**). PHOM score, age, sex, Karnofsky Performance Status (KPS), Charlson Comorbidity Index (CCI), overall stage, and post radiation chemotherapy were included as covariates in a Cox Proportional Hazards Model for overall and cancer specific survival.

This cohort was divided into 2 groups by median PHOM score (PHOM $= -0.0372$) to compare trends in overall survival and trends in cumulative incidence by disease specific death. Kaplan Meier curves were drawn to compare overall survival between the two groups, and log-rank statistics were used to compare the survival trends. Cumulative incidence curves were drawn to compare cause of death between these 2 groups.

This analysis was repeated with optimized tertiles. Tertiles were calculated by selecting the two PHOM score cutoff values that resulted in the maximal chi square value of the Kaplan Meier Curve. The low risk group (n = 211) was defined as below -0.460, medium risk group (n = 172) as between -0.460 and 0.668, and high risk group (n = 171) as above 0.668. Both Kaplan

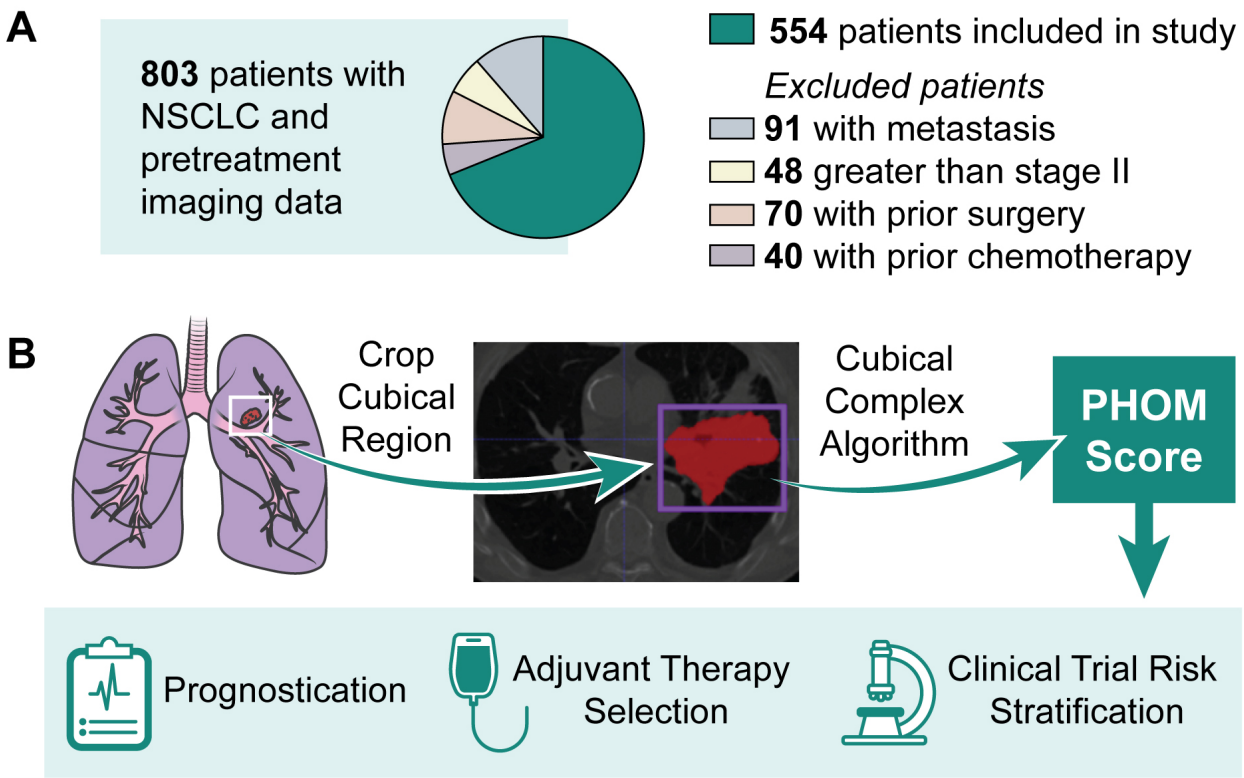

Figure 1. **Conceptual Overview of Translating Utility of PHOM Score.** **(A)** 803 patients were in our database with imaging and clinical data for NSCLC treated primarily with SBRT. 249 patients were excluded based on their stage or treatment history. **(B)** The PHOM Score is algorithmically calculated from a tumor segmented by a clinician. Note, this particular cross section demonstrates a large tumor greater than stage II but was selected for visualization purposes. Only stage II tumors and below were selected for analysis. **(C)** We envision the PHOM Score to have utility in prognostication, therapy selection, and risk stratification.

Meier curves and cumulative incidence curves were drawn for these three groups. The Benjamini-Hochberg correction was used to correct for multiple comparisons for the Kaplan Meier pairwise comparisons.

The multivariable Cox proportional hazards model for overall survival formed the basis of a nomogram to predict 1, 2, 5, and 8 year survival. Predicted median survival was calculated as a weighted sum of the individual survival predictions. This model was internally validated using bootstrap resampling (1,000 repetitions), and calibration curves were checked to ensure alignment of observed and optimism fitted survival rates. To assess the relative contribution of each covariate towards prediction ability of the multivariable Cox model for overall survival, the drop in C index was calculated by omitting each covariate one at a time from the full model. The C index has been routinely used to evaluate the discriminating ability of a survival model[13]. All data were processed and analyzed using R (v3.6.1) and Python (v3.7.6) [14–16]. Anonymized data may be requested from the authors. Code with explanation for this data pipeline can be found at `https://github.com/eashwarsoma/phom-lungca-ccf`.

3 Results

The patients in this study were generally able bodied individuals with early stage NSCLC and a moderate number of comorbidities. **Table 1** provides a descriptive overview of the patient population. All patients had stage I or II primary non-small cell lung cancer (none had nodal disease). No patients in this cohort had treatment prior to stereotactic body radiation therapy (SBRT), but 26 patients (4.7%) had some form of post SBRT chemotherapy. KPS scores in this study ranged from $50-100$. Most patients had baseline independent functional status corresponding to a Karnofsky Performance Status (KPS) of 80 (215 patients) and $90-100$ (168 patients). Using an α/β ratio of 10, mean dose received over treatment course was $100.54Gy$ (SD: $25.24Gy$) EQD2. 89 patients had minimal comorbidity corresponding to a Charlson Comorbidity Index (CCI) of $2-4$. Most patients had additional comordbities with scores ranging from $5-8$. 60 patients had severe comorbidity (CCI >8). 115 (20.8%) patients died from cancer, and 323 (58.3%) patients died from other causes. 116 patients (20.9%) were alive at last follow up, and the median follow up time for those alive was approximately 4.7 years (SD: 2.14 years).

Patient Characteristics

Label	level	Overall
n		554
Age, mean (SD)		74.35 (9.15)
Sex, mean (SD)	Male	263 (47.5)
	Female	291 (52.5)
Race (%)	Black	79 (14.3)
	White	459 (82.9)
	Other	16 (2.9)
Years Smoked, mean (SD)		52.25 (33.89)
EQD2, mean (SD)		100.54 (25.24)
Post SBRT Therapy (%)	No	528 (95.3)
	Yes	26 (4.7)
Overall Stage (%)	IA	363 (65.5)
	IB	121 (21.8)
	IIA	44 (7.9)
	IIB	26 (4.7)
Karnofsky Performance Status (%)	KPS = 50-60	44 (7.9)
	KPS = 70	127 (22.9)
	KPS = 80	215 (38.8)
	KPS = 90-100	168 (30.3)
Charlson Comorbidity Index (%)	CCI = 2-4	89 (16.2)
	CCI = 5	125 (22.7)
	CCI = 6	114 (20.7)
	CCI = 7	99 (18.0)
	CCI = 8	64 (11.6)
	CCI = 9-14	60 (10.9)
Followup Time, mean (SD)		56.37 (25.72)

Table 1. Patient Characteristics of Study Cohort. Patients in this cohort had early stage tumors, were generally healthy (high KPS), and had a moderate number of comorbidities (CCI: 5-8). 554 patients were present in the cohort. Followup time describes the mean number of months between treatment and most recent followup appointment for patients who were alive. EQD2: Equivalent Dose In 2-Gy Fractions, calculated using an α/β ratio of 10. KPS: Karnofsky Performance Score CCI: Charlson Comorbidity Index

PHOM score was a significant predictor of both overall survival (HR: 1.17; 95% CI: $1.07-1.28$, $p < 0.001$) and cancer specific survival (HR: 1.31; 95% CI: $1.11-1.56$, $p = 0.0014$) after controlling for age, functional status, comorbidity, treatment factors and stage. For cancer specific survival, the PHOM score was the only significant covariate in the multivariable model. **Figure 2** shows a forest plot of variable significance in a Cox Proportional Hazards Model for overall and cancer specific survival, and **Table 2** lists exact hazard ratios. For overall survival, high functional status of KPS $= 90-100$ was protective for survival (HR: 0.46, 95% CI: $0.32-0.67$, $p < 0.001$). Increased comorbidity was also associated with poor overall survival in the multivariable model (HR: 2.54, 95% CI: $1.69-3.80$, $p < 0.001$). **Supplemental Table 1** shows the p-values for the Cox Proportional Hazards models.

The PHOM score produced well defined risk categories for overall survival and cancer death incidence when stratified by median or optimized cutoff values. **Figure 3A** describes the survival differences by PHOM score groups stratified by the cohort's median PHOM score. Patients in high PHOM group had significantly worse survival ($p < 0.001$) compared to patients in low PHOM score group. Patients in the low PHOM score group had a median survival of 45.41 months (95% CI: $40.08-51.78$), which was significantly higher compared to patients in the higher PHOM score group (median: 29.18 months, 95% CI: $23.62-34.27$, $p < 0.001$). We next hypothesized that the PHOM score could delineate risk groups at higher resolution, and so chose two cutpoints of PHOM score to optimally separate the cohort into three groups of low, intermediate and high probability of death. **Figure 3B** describes the survival differences predicted by these optimized PHOM score risk groups. The median survival for the high PHOM risk group was 25.73 months (95% CI: $20.86-31.02$). The median survival for the medium and low risk groups were 34.83 months (95% CI: $29.93-44.85$) and 47.02 months (95% CI: $40.90-58.05$) respectively. These groups had significant differences in overall survival; however, reporting the p-value is somewhat moot as the cutoffs were calculated by optimizing the chi square value of the Kaplan Meier curve.

PHOM score strata delineates cancer specific death incidence curves but not death incidence curves due to other causes.

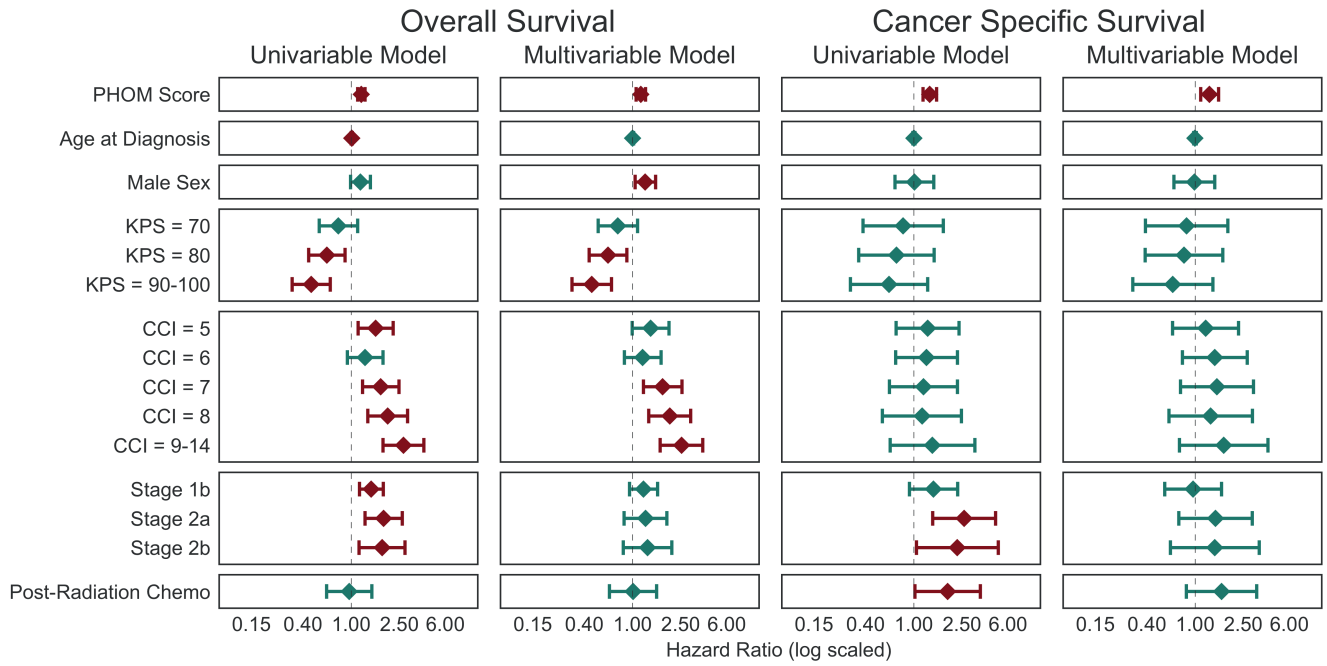

Figure 2. Forest Plot of Overall and Cancer Specific Cox Proportional Hazards Models. The PHOM Score was the only significant covariate for both overall and cancer specific survival. Bands represent 95% confidence intervals. The red bars represent significant hazard ratios. KPS (Karnofsky performance status) is compared against KPS $= 50-60$. CCI (Charlson Comorbidity Index) is compared against CCI $= 2-4$. Stage covariates are compared against Stage 1a.

Cox Proportional Hazards Model

	Overall Survival UV Hazard Ratio	Overall Survival MV Hazard Ratio	Cancer Specific Survival UV Hazard Ratio	Cancer Specific Survival MV Hazard Ratio
PHOM Score	**1.21 (1.13-1.30)**	**1.17 (1.07-1.28)**	**1.35 (1.19-1.54)**	**1.31 (1.11-1.56)**
Age at Diagnosis	**1.01 (1.00-1.02)**	1.00 (0.99-1.02)	1.00 (0.98-1.02)	0.99 (0.97-1.02)
Male Sex	1.19 (0.99-1.44)	**1.27 (1.05-1.55)**	1.01 (0.70-1.46)	0.98 (0.67-1.45)
KPS = 70	0.78 (0.54-1.13)	0.76 (0.52-1.10)	0.81 (0.38-1.75)	0.85 (0.39-1.86)
KPS = 80	**0.63 (0.45-0.89)**	**0.63 (0.44-0.90)**	0.72 (0.35-1.47)	0.81 (0.39-1.69)
KPS = 90-100	**0.47 (0.33-0.67)**	**0.46 (0.32-0.67)**	0.62 (0.30-1.30)	0.65 (0.30-1.40)
CCI = 5	**1.59 (1.14-2.22)**	1.41 (0.99-2.00)	1.30 (0.71-2.36)	1.22 (0.65-2.28)
CCI = 6	1.30 (0.93-1.83)	1.21 (0.86-1.72)	1.27 (0.71-2.29)	1.45 (0.78-2.69)
CCI = 7	**1.75 (1.24-2.48)**	**1.77 (1.23-2.56)**	1.20 (0.63-2.29)	1.51 (0.76-3.03)
CCI = 8	**2.00 (1.37-2.92)**	**2.03 (1.36-3.02)**	1.17 (0.55-2.47)	1.34 (0.61-2.97)
CCI = 9-14	**2.70 (1.83-3.98)**	**2.54 (1.69-3.80)**	1.42 (0.64-3.19)	1.72 (0.74-3.99)
Post-Radiation Chemo	0.96 (0.63-1.48)	1.01 (0.64-1.58)	**1.90 (1.02-3.54)**	1.65 (0.84-3.22)
Stage 1b	**1.46 (1.17-1.84)**	1.23 (0.94-1.61)	1.45 (0.92-2.30)	0.96 (0.56-1.65)
Stage 2a	**1.85 (1.30-2.64)**	1.28 (0.85-1.92)	**2.60 (1.43-4.73)**	1.47 (0.73-2.96)
Stage 2b	**1.80 (1.16-2.78)**	1.33 (0.84-2.11)	**2.28 (1.05-4.98)**	1.45 (0.62-3.38)

Table 2. Cox Proportional Hazards Model for Overall and Cancer Specific Survival. The PHOM Score was a significant covariate for survival even after controlling for clinical variables. KPS and CCI were significant covariates for overall survival but not in cancer specific survival. Values are given as hazard ratio (95% Confidence Interval). KPS (Karnofsky Performance Status) is compared against KPS $= 50-60$. CCI (Charlson Comorbidity Index) is compared against CCI of $2-4$. Stage covariates are compared against Stage 1a. Bolded values are statistically significant with $p < 0.05$. P-values for this table are included as **Supplemental Table 1**.

Figure 4A compares cause specific death between PHOM score groups divided by cohort median. Having an above median PHOM score was associated with a 0.244 (95% CI: $0.192-0.296$) chance of cancer specific death by month 65, which was significantly higher compared to the below median PHOM score chance of death at 0.171 (95% CI: $0.123-0.218$, $p = 0.029$).

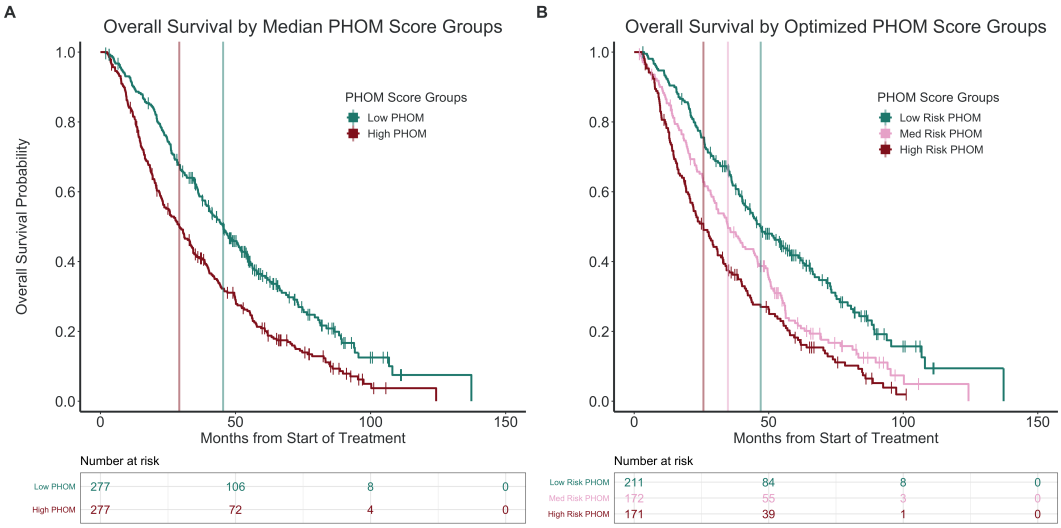

Figure 3. Kaplan Meier Overall Survival by PHOM Score. Stratifying the cohort by median PHOM score groups and optimized cutoffs produced well demarcated survival curves. **(A)** The median survival for the high PHOM group was 29.18 months (95% CI: 23.62 – 34.27). The median survival for the low PHOM group was significantly higher at 45.41 months (95% CI: 40.08 – 51.78, $p < 0.001$). **(B)** The median survival for the high PHOM risk group was 25.73 months (95% CI: 20.86 – 31.02). This was significantly less than both the medium ($p = 0.020$) and low risk PHOM score groups ($p < 0.001$). The median survival for the medium risk group was 34.83 months (95% CI: 29.93 – 44.85). This was significantly less than the low risk PHOM score group ($p < 0.001$). The median survival for the low risk group was 47.02 months (95% CI: 40.90 – 58.05). However, it is important to note that these p-values are somewhat moot since the tertiles were calculated to maximize the chi square value of the KM curve.

However, for other causes of death, a high vs low PHOM score corresponded to a nonsignificant 0.582 (95% CI: 0.521 – 0.642) vs 0.499 (95% CI: 0.436 – 0.563) chance of death by month 65. **Figure 4B** compares cause specific death among PHOM score groups divided by optimized PHOM score risk groups. Similarly, we found similar stratification of cancer specific death but not due to other causes among the three risk groups. For low, medium, and high risk PHOM score groups, the chance of cancer death by month 65 was 0.146 (95% CI: 0.0950 – 0.197), 0.194 (95% CI: 0.133 – 0.255), and 0.296 (95% CI: 0.224 – 0.366) respectively. For low, medium, and high risk PHOM score groups, the chance of death from other causes by month 65 was 0.474 (95% CI: 0.401 – 0.546), 0.612 (95% CI: 0.535 – 0.689), and 0.551 (95% CI: 0.474 – 0.629) respectively. 115 patients in this cohort died of cancer specific death of which 80 were due to nodal and distal progression and the remaining 35 due to new primary, local, or lobar progression.

We drew nomograms, which are user friendly visual tools that represent the underlying survival regression models. Nomograms were calibrated for 1, 2, 5, and 8-year overall survival. The model was internally validated using bootstrap resampling (1,000 repetitions), and calibration curves are shown in **Supplemental Figure 1**. The apparent and optimism bias corrected curves showed relatively strong alignment with the ideal curve indicating that our model is internally valid and not overfitted. **Supplemental Figure 2** demonstrates the relative contribution of each covariate to the predictive ability of the multivaraite Cox model with relative drop in C index.

Each covariate from the multivariable Cox Proportional Hazards Model is associated with a certain point value, and summing the point values for a given patient's parameter generates a score that can be used to assign 1, 2, 5, and 8 year overall survival chance. The weighted sum of these survival chances gives the predicted median survival. An online interactive version of this nomogram is available at `https://eashwarsoma.shinyapps.io/LungCancerTDATest/`.

4 Discussion

The PHOM score is predictive of patient outcome and adding it to a nomogram of clinical variables improves overall survival predication in patients with NSCLC treated with SBRT. We show our novel topologically inspired radiomics variable serves as a useful metric to assist patients in understanding their prognosis, clinicians in selecting treatments, and potentially clinical trialists in risk stratifying for clinical trials. To our knowledge, there is currently no similar metric that can describe risk and survival in patients who receive primary treatment with SBRT.

Stratifying PHOM score by median groups reveals worse overall and cancer specific survival in high PHOM score group. However, the high PHOM score group is not associated with death due to non-cancer causes. By differentiating cancer-specific survival from death due to other causes, we show that the PHOM score is reflective of cancer severity (**Figure 3** and **Figure 4**). Similarly, our risk category tertile groups demonstrate worse overall and cancer specific survival among the high risk groups. Most cancer deaths were due to nodal and distal progression suggesting a higher PHOM score could indicate a need for

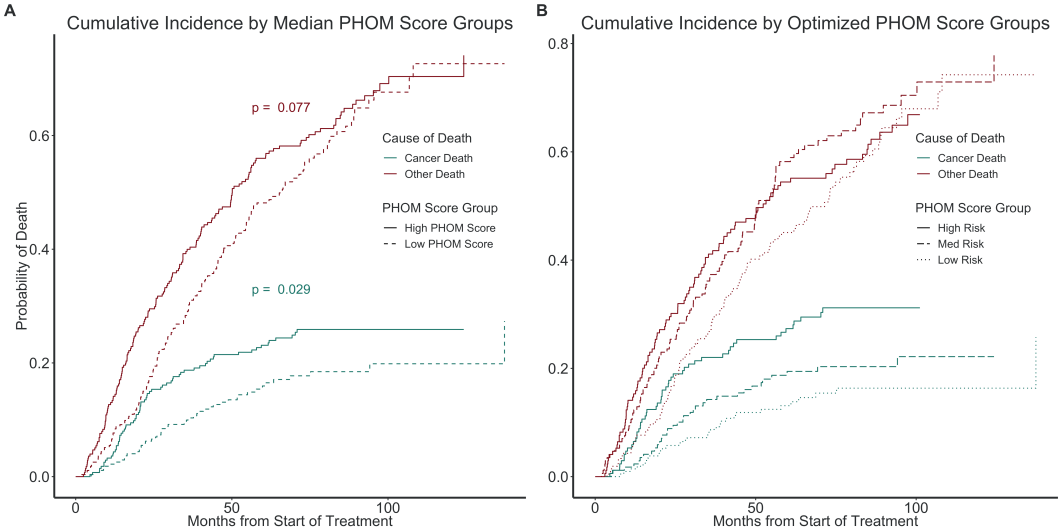

Figure 4. **Cumulative Incidence of Death by Specific Cause** Stratifying the cohort by median PHOM score groups and optimized cutoffs produced well demarcated cumulative incidence curves for cancer specific death but not death due to other causes. **(A)** Having an above median PHOM score was associated with a 0.244 (95% CI: 0.192 – 0.296) chance of cancer specific death by month 65. A below median PHOM score was associated with a significantly less chance of death by month 65 at 0.171 (95% CI: 0.123 – 0.218, $p = 0.029$). However, for other causes of death, a high vs low PHOM score corresponds to a nonsignificant 0.582 (95% CI: 0.521 – 0.642) vs 0.499 (95% CI: 0.436 – 0.563) chance of death by month 65. **(B)** For low, medium, and high risk PHOM score groups, the chance of cancer death by month 65 was 0.146 (95% CI: 0.0950 – 0.197), 0.194 (95% CI: 0.133 – 0.255), and 0.296 (95% CI: 0.224 – 0.366) respectively. For low, medium, and high risk PHOM score groups, the chance of death from other causes by month 65 was 0.474 (95% CI: 0.401 – 0.546), 0.612 (95% CI: 0.535 – 0.689), and 0.551 (95% CI: 0.474 – 0.629) respectively. Similarly, the difference among incidence of death at month 65 was significant when assessing cancer death ($p = 0.0013$) but not other death. 115 patients in this cohort died of cancer specific death of which 80 were due to nodal and distal progression and the remaining 35 due to new primary, local, or lobar progression. The p-values are moot similar to the Kaplan-Meier risk stratification analysis since we maximized over the chi square value of the KM curve.

adjuvant therapy. As mentioned earlier, the PHOM score may be used by trialists in risk stratifying, and we offer our tertile groups as one possible method of stratification.

In our cancer-specific survival Cox models, KPS and CCI do not affect cancer-specific survival in the multivariable model, which is expected as these variables measure overall health rather than tumor progression (**Table 2**). The PHOM score is the only significant predictor for cancer specific survival in the multivariable model. Stage did not contribute to predicting survival in the multivariable models, possibly due to high local control rates when early stage tumors are treated with SBRT[17].

The KPS had the greatest drop in C index score, and CCI and PHOM score resulted in similar C index drops. This roughly reflects the importance these metrics have in the predictive power of overall survival (**Supplemental Table 2**). We postulate in our model that PHOM drives prediction of cancer specific death whereas CCI and KPS drive prediction of death from other causes. Since these cancers are treated early stage, patients tend to die from comorbidities, so it was improtant to include large picture clinical variables like CCI and KPS in our model. The overlapping of the calibration curves of apparent, bias-corrected, and ideal survival demonstrate strong internal validity of our predictive overall survival nomogram (**Supplemental Figure 1**).

To our knowledge, this is the first paper that utilizes persistent homology of CT scans to predict overall survival in lung cancer. We have built on our prior work where we developed the PHOM score[12]. However, our prior work was limited to demonstrating statistical association with overall survival and did not include important covariates such as KPS and CCI due to limitations in available data. We speculate our metric is a measure of underlying structural tissue heterogeneity. Increased tissue heterogeneity is a possible sign of a more aggressive tumor which is why our metric correlates well with cancer specific survival and predicts overall survival. This increased tissue heterogeneity can manifest in CT imaging findings that we believe the PHOM score is capturing as a higher risk early stage tumor. Our new imaging persistent homology metric adds to the other metrics that have been developed for glioblastoma, breast, and prostate cancer clinical outcomes research[8,10,18].

Persistent homology has opened up an entirely new suite of tools for radiomics analysis of imaging data. In particular, results based on the PHOM score have strong external validity as the same score was previously significantly associated with NSCLC survival in the publicly available The Cancer Imaging Archive dataset[12], and here is a significant predictor of NSCLC survival in a distinct dataset. Traditional radiomics features have been used to predict tumor histology and needed dose to prevent cancer recurrence[19,20]. Topology is not currently a standard variable in radiomics, so it is not known how it could interact. We have shown that the PHOM score independently predicts survival in NSCLC even after controlling for traditional clinical metrics. How the PHOM score could interact with traditional Radiomic measures that have already demonstrated clinical utility in NSCLC remains to be answered. Additionally, the PHOM score could be incorporated with

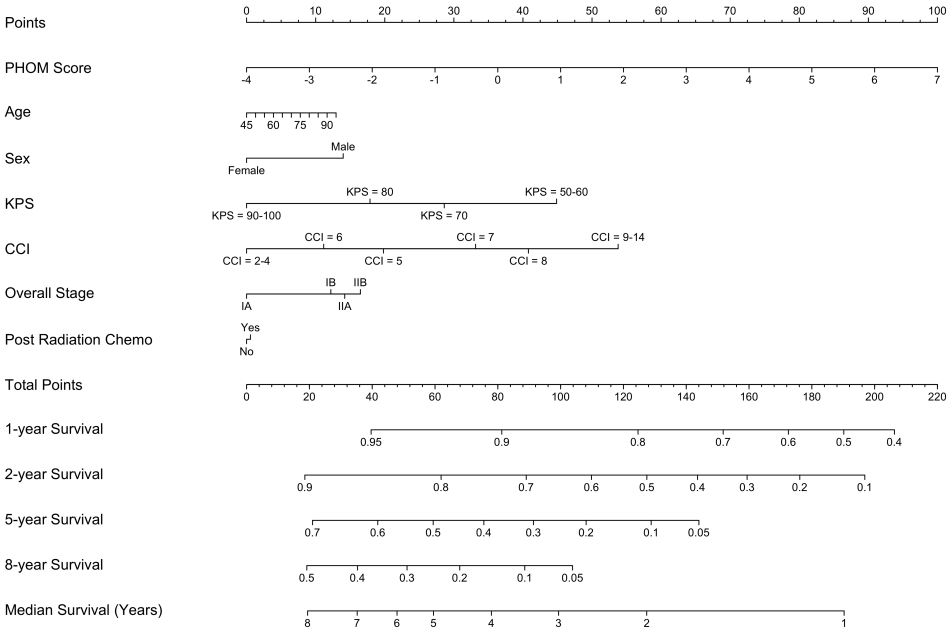

Figure 5. Nomogram for Overall Survival. This nomogram is a visual tool to convert the variables in our Cox overall survival model into a common risk score. This risk score can then convert into predicted survival. An online interactive version of this nomogram is available at https://eashwarsoma.shinyapps.io/LungCancerTDATest/. KPS: Karnofsky Performance Status. CCI: Charlson Comorbdity Index.

other non imaging data. Genomic models such as the genomically adjusted radiation dose (GARD) have been developed to predict individualized response to different radiation doses[21] and have been found to be predictive of individual patient outcome in a large meta-analysis[22]. We forsee future clinical models that incorporate genomic, imaging, and other modalities of data to more precisely guide therapy.

While our results are promising for NSCLC, some limitations must be considered. Primarily, our nomogram is only validated for patients with early stage NSCLC who receive SBRT therapy as their primary treatment modality with no surgery or prior chemotherapy. Therefore, this calculator is not yet valid for patients with lung resections, which is a common procedure in lung cancer patients. Additionally, we could not generate a cancer specific survival curve due to poor calibration curves when validating such a model. We believe this to be a result of the limited number of cancer specific deaths in this cohort, likely due to the fact that all patients had treated early stage lung cancer. Publicizing this nomogram, recruiting data from other institutions, and conducting prospective studies with longer follow up could address these limitations in future studies. Additionally, future studies could analyze how the PHOM score fits in with traditional radiomics characteristics. The widespread imaging capability of modern hospitals makes imaging analysis such as computing the PHOM score practical to utilize in daily patient care. In cohort studies or randomized controlled trials, the PHOM score could be used to stratify patients into risk categories to investigate who might benefit from adjuvant therapy. Long term, we envision the creation of a risk calculator that extracts the most useful features of an imaging data that can both prognosticate and help make clinical decisions.

Acknowledgments

The authors thank members of Theory Division for their constructive feedback and valuable input in this project. We thank Jessica Scarborough, PhD for advice and code to generate optimal PHOM score tertiles. JGS was supported by NIH grant R37 CA244613 and the American Cancer Society through their Research Scholar Grant. ES and RRW were supported by the Case Comprehensive Cancer Center Summer Training Grant for medical students. KY was supported by the Computational Genomic Epidemiology of Cancer (CoGEC) Program at Case Comprehensive Cancer Center (T32CA094186), Young Investigator Award from ASCO Conquer Cancer Foundation, and RSNA Research Resident Grant.

Author contributions statement

All authors made substantial contributions to: (1) the conception and design of the study or acquisition, analysis, and interpretation of the data; (2) draft the article or revising it critically for important intellectual content; (3) final approval of the submitted version.

References

1. Siegel, R. L., Miller, K. D. & Jemal, A. Cancer statistics, 2020. *CA: A Cancer J. for Clin.* **70**, 7–30, DOI: 10.3322/caac.21590 (2020).
2. Duma, N., Santana-Davila, R. & Molina, J. R. Non–small cell lung cancer: Epidemiology, screening, diagnosis, and treatment. *Mayo Clin. Proc.* **94**, 1623–1640, DOI: 10.1016/j.mayocp.2019.01.013 (2019).
3. Chang, J. Y. *et al.* Stereotactic ablative radiotherapy for operable stage i non-small-cell lung cancer (revised STARS): long-term results of a single-arm, prospective trial with prespecified comparison to surgery. *The Lancet Oncol.* **22**, 1448–1457, DOI: 10.1016/s1470-2045(21)00401-0 (2021).
4. Goldstraw, P. *et al.* The IASLC lung cancer staging project: Proposals for revision of the TNM stage groupings in the forthcoming (eighth) edition of the TNM classification for lung cancer. *J. Thorac. Oncol.* **11**, 39–51, DOI: 10.1016/j.jtho.2015.09.009 (2016).
5. Sperduto, P. W. *et al.* Estimating survival in patients with lung cancer and brain metastases. *JAMA Oncol.* **3**, 827, DOI: 10.1001/jamaoncol.2016.3834 (2017).
6. Gillies, R. J., Kinahan, P. E. & Hricak, H. Radiomics: Images are more than pictures, they are data. *Radiology* **278**, 563–577, DOI: 10.1148/radiol.2015151169 (2016).
7. Carlsson, G. Topology and data. *Bull. Am. Math. Soc.* **46**, 255–308 (2009).
8. Gordetsky, J. & Epstein, J. Grading of prostatic adenocarcinoma: current state and prognostic implications. *Diagn. Pathol.* **11**, DOI: 10.1186/s13000-016-0478-2 (2016).
9. AI, B. & Oncology, C. C. C. *Comparative Oncology* (Bucharest: The Publishing House of the Romanian Academy, 2007).
10. Crawford, L., Monod, A., Chen, A. X., Mukherjee, S. & Rabadán, R. Predicting clinical outcomes in glioblastoma: An application of topological and functional data analysis. *J. Am. Stat. Assoc.* 1–12, DOI: 10.1080/01621459.2019.1671198 (2019).
11. Oyama, A. *et al.* Hepatic tumor classification using texture and topology analysis of non-contrast-enhanced three-dimensional t1-weighted MR images with a radiomics approach. *Sci. Reports* **9**, DOI: 10.1038/s41598-019-45283-z (2019).
12. Somasundaram, E., Litzler, A., Wadhwa, R., Owen, S. & Scott, J. Persistent homology of tumor CT scans is associated with survival in lung cancer. *Med. Phys.* **48**, 7043–7051 (2021).
13. Pencina, M. J. & D'Agostino, R. B. OverallC as a measure of discrimination in survival analysis: model specific population value and confidence interval estimation. *Stat. Medicine* **23**, 2109–2123, DOI: 10.1002/sim.1802 (2004).
14. R Core Team. *R: A Language and Environment for Statistical Computing*. R Foundation for Statistical Computing, Vienna, Austria (2012). ISBN 3-900051-07-0.
15. RStudio Team. *RStudio: Integrated Development Environment for R*. RStudio, PBC., Boston, MA (2020).
16. Van Rossum, G. & Drake, F. L. *Python 3 Reference Manual* (CreateSpace, Scotts Valley, CA, 2009).
17. Sebastian, N. T., Xu-Welliver, M. & Williams, T. M. Stereotactic body radiation therapy (SBRT) for early stage non-small cell lung cancer (NSCLC): contemporary insights and advances. *J. Thorac. Dis.* **10**, S2451–S2464, DOI: 10.21037/jtd.2018.04.52 (2018).
18. Nicolau, M., Levine, A. J. & Carlsson, G. Topology based data analysis identifies a subgroup of breast cancers with a unique mutational profile and excellent survival. *Proc. Natl. Acad. Sci.* **108**, 7265–7270, DOI: 10.1073/pnas.1102826108 (2011).
19. Woody, N. M. *et al.* A histologic basis for the efficacy of SBRT to the lung. *J. Thorac. Oncol.* **12**, 510–519, DOI: 10.1016/j.jtho.2016.11.002 (2017).
20. Lou, B. *et al.* An image-based deep learning framework for individualising radiotherapy dose: a retrospective analysis of outcome prediction. *The Lancet Digit. Heal.* **1**, e136–e147, DOI: 10.1016/s2589-7500(19)30058-5 (2019).
21. Scott, J. G. *et al.* A genome-based model for adjusting radiotherapy dose (GARD): a retrospective, cohort-based study. *The Lancet Oncol.* **18**, 202–211, DOI: 10.1016/s1470-2045(16)30648-9 (2017).
22. Scott, J. G. *et al.* Pan-cancer prediction of radiotherapy benefit using genomic-adjusted radiation dose (gard): a cohort-based pooled analysis. *The Lancet Oncol.* **22**, 1221–1229 (2021).

Supplemental Information

Supplemental Table 1 shows the hazard ratios for our Cox proportional-hazards models with p-values. The PHOM score was the only covariate that was significant in all four models suggesting it is a predictor of overall and cancer survival.

Cox Proportional Hazards Model

	Overall Survival Univariable Model		Overall Survival Multivariable Model		Cancer Specific Survival Univariable Model		Cancer Specific Survival Multivariable Model	
	Hazard Ratio	p-value	Hazard Ratio	p-value	Hazard Ratio	p-value	Hazard Ratio	p-value
PHOM Score	1.21 (1.13-1.30)	< 0.001	1.17 (1.07-1.28)	< 0.001	1.35 (1.19-1.54)	< 0.001	1.31 (1.11-1.56)	0.0014
Age at Diagnosis	1.01 (1.00-1.02)	0.0077	1.00 (0.99-1.02)	0.46	1.00 (0.98-1.02)	0.96	0.99 (0.97-1.02)	0.61
Male Sex	1.19 (0.99-1.44)	0.067	1.27 (1.05-1.55)	0.017	1.01 (0.70-1.46)	0.95	0.98 (0.67-1.45)	0.94
KPS = 70	0.78 (0.54-1.13)	0.18	0.76 (0.52-1.10)	0.14	0.81 (0.38-1.75)	0.6	0.85 (0.39-1.86)	0.68
KPS = 80	0.63 (0.45-0.89)	0.0087	0.63 (0.44-0.90)	0.011	0.72 (0.35-1.47)	0.37	0.81 (0.39-1.69)	0.57
KPS = 90-100	0.47 (0.33-0.67)	< 0.001	0.46 (0.32-0.67)	< 0.001	0.62 (0.30-1.30)	0.21	0.65 (0.30-1.40)	0.27
CCI = 5	1.59 (1.14-2.22)	0.0069	1.41 (0.99-2.00)	0.055	1.30 (0.71-2.36)	0.4	1.22 (0.65-2.28)	0.54
CCI = 6	1.30 (0.93-1.83)	0.12	1.21 (0.86-1.72)	0.28	1.27 (0.71-2.29)	0.42	1.45 (0.78-2.69)	0.24
CCI = 7	1.75 (1.24-2.48)	0.0015	1.77 (1.23-2.56)	0.0022	1.20 (0.63-2.29)	0.58	1.51 (0.76-3.03)	0.24
CCI = 8	2.00 (1.37-2.92)	< 0.001	2.03 (1.36-3.02)	< 0.001	1.17 (0.55-2.47)	0.69	1.34 (0.61-2.97)	0.47
CCI = 9-14	2.70 (1.83-3.98)	< 0.001	2.54 (1.69-3.80)	< 0.001	1.42 (0.64-3.19)	0.39	1.72 (0.74-3.99)	0.21
Had Post-Radiation Chemo	0.96 (0.63-1.48)	0.86	1.01 (0.64-1.58)	0.97	1.90 (1.02-3.54)	0.043	1.65 (0.84-3.22)	0.14
Stage 1b	1.46 (1.17-1.84)	< 0.001	1.23 (0.94-1.61)	0.12	1.45 (0.92-2.30)	0.11	0.96 (0.56-1.65)	0.88
Stage 2a	1.85 (1.30-2.64)	< 0.001	1.28 (0.85-1.92)	0.24	2.60 (1.43-4.73)	0.0017	1.47 (0.73-2.96)	0.28
Stage 2b	1.80 (1.16-2.78)	0.0082	1.33 (0.84-2.11)	0.23	2.28 (1.05-4.98)	0.038	1.45 (0.62-3.38)	0.39

Supplemental Table 1. Cox Proportional Hazards Model for Overall and Cancer Specific Survival with p-values. Values given as Hazard ratio (95% Confidence Interval). KPS (Karnofsky performance status) is compared against KPS > 70. CCI (Charlson Comorbidity Index) is compared against CCI of 1-4. Stage covariates are compared against Stage 1a. This is the same table as P-values for this table are included as **Table 2** with p-values added.

Supplemental Table 2 shows the chi-square goodness of fit statistic for univariable Cox proportional-hazards model for overall survival and for the full multivariable model. The rightmost column demonstrates the drop in C-index when each variable is omitted from the full model. Larger positive numbers drops indicate that particular variable contributes relatively more to the predictive ability of the model. Importantly, omitting one covariate at a time also tells us whether that covariate provides redundant predictive information. Since PHOM Score, KPS, and CCI resulted in the largest drops in C-index, these variables give the most predictive information in the multivariable Cox-proportional hazards survival model.

We internally validated the Cox models using bootstrap resampling. The apparent performance reflects the original model performance on boot strap samples. The bias-corrected performance represents the performance of the same multivariable Cox model but recalculated using a boot strap sample. The primary function of the bias-corrected line is to show our model's

	C index	Chi-Square	Drop in C index
KPS	0.6044	21.4200	0.0186
PHOM Score	0.6167	12.6000	0.0064
CCI	0.6166	29.8900	0.0064
Sex	0.6243	5.7460	-0.0013
Overall Stage	0.6258	3.4120	-0.0027
Age	0.6258	0.5512	-0.0028
Post Radiation Chemo	0.6260	0.0018	-0.0030
Full Model	0.6230	94.2500	0.0000

Supplemental Table 2. Goodness of Fit and Predictive Ability of Each Variable for Overall Survival Cox Model. C-index is a measure of assessing whether the risk predicted by the model is associated with reduced survival[13]. The bottom row gives values for the full model, and each row describes the change in the C index from the full model if that variable were omitted. The second column gives the chi-square value for a univariable Cox model of the row variable, and the last row provides the full model.

prediction is not the result of overfitting on our data. Relative overlap between the apparent and bias-corrected lines along the ideal line (the hypothetical perfect model) represents strong internal validity of our model.

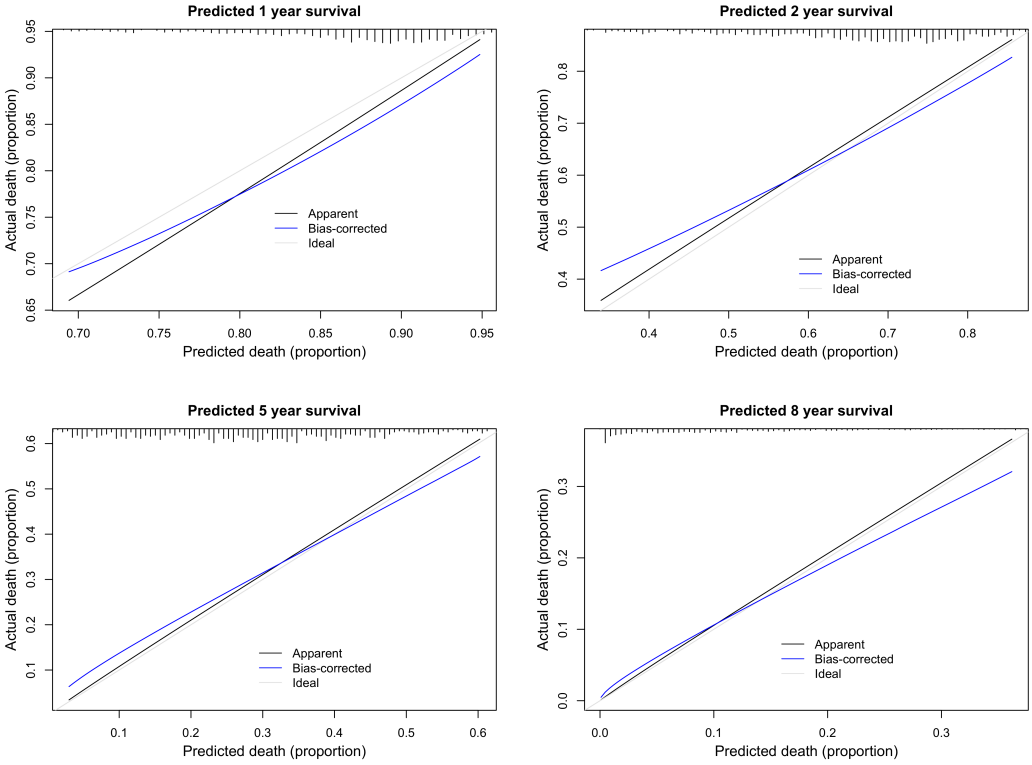

Supplemental Figure 1. Calibration Curves for Overall Survival Cox Proportional Hazards Model. The apparent calibration line represents represents the performance of our model on the original data set. Bias corrected curves were calculated through 1000 bootstrap resamples. For each bootstrap sample, a new Cox model using the bootstrap sample was generated. Optimism was calculated as the difference between the performance of the real sample on the bootstrap Cox model and the performance of the bootstrap sample on the bootstrap Cox model. The optimism estimate from each bootstrap resample were averaged and subtracted from the apparent performance curve to generate the bias corrected curve. This bias corrected curve aligning with the apparent and ideal curves is an indication that our model is not overfitted.